SWITCHING ON THE SOMMERFELD HALF-LINE DIFFRACTION PROBLEM

David P. Hewett[†,‡,*], **John R. Ockendon**[†], **David J. Allwright**[†]
[†]Oxford Centre for Industrial and Applied Mathematics, University of Oxford, Oxford, UK
[‡]Present address: Department of Mathematics and Statistics, University of Reading, Reading, UK
[*]Email: d.p.hewett@reading.ac.uk

Talk Abstract

This paper concerns the switching on of two-dimensional time-harmonic scalar waves. We consider the diffraction of a time-harmonic plane wave by a half-line, determining the rate at which the solution of the time domain 'switching on' problem converges to the solution of the corresponding frequency domain problem (the classical 'Sommerfeld problem') as the time since the wave was switched on goes to infinity. The rate of convergence is found to be dependent both on the strength of the singularity on the leading wavefront, and on the observation point. In the case of grazing incidence the frequency domain solution is immediately attained along the shadow boundary after the arrival of the leading wavefront. The case of non-grazing incidence is also considered.

Introduction

In the study of linear wave propagation (e.g. acoustic, elastic or electromagnetic waves) one often considers idealised time-harmonic (or 'frequency domain') solutions, which represent waves with a single frequency of temporal oscillation. When a source of time-harmonic waves is switched on, one might expect that as the time since the source was switched on increases, the resulting time-dependent wave field should converge to the solution of the corresponding frequency domain problem, in which the source has 'always been on'. This is usually referred to as the Limiting Amplitude Principle (LAP).

Whether or not the LAP holds, and the rate at which the frequency domain solution is attained, depend on the nature of the source, the domain in which the waves propagate, and the observation point. It is well-known that the LAP holds in the case of scattering by smooth obstacles of fields due to smooth source distributions (see e.g. [1]-[3]). The case where the scatterer possesses boundary singularities has not been studied in such detail, although in a recent publication [4] the LAP has been proved for the scattering of a plane wave by a wedge. However, the analysis of [4] did not extend to the calculation of the rate of convergence to the frequency domain solution.

The aim of this paper is to provide a detailed analysis of this rate of convergence in the special case where the scatterer is a half-line. To the best of our knowledge, this is the first such analysis for a non-smooth scatterer. Our analysis is based on direct asymptotic analysis of the explicit exact solutions of the relevant time domain and frequency domain problems. (Further details of the results presented here can be found in [5].)

Problem statement

The half-line scatterer is described in Cartesian coordinates (x, y) by $y = 0, x \geq 0$. The time domain diffraction problem we consider comprises the scalar wave equation

$$\frac{\partial^2 \Phi}{\partial t^2} - c_0^2 \nabla^2 \Phi = 0, \quad 0 < r < \infty, \quad 0 < \theta < 2\pi, \quad (1)$$

where (r, θ) are the usual polar coordinates, along with the rigid (Neumann) boundary condition

$$\frac{\partial \Phi}{\partial \theta} = 0, \qquad 0 < r < \infty, \quad \theta \in \{0, 2\pi\}, \qquad (2)$$

and a suitable prescription of the 'switched on' incident plane wave. We consider first the simplest case in which the wave is incident from the direction $\theta_0 = 0^+$ (the general case will be discussed later), with

$$\Phi = H(\pi - \theta) G(t + x/c_0), \qquad t < 0, \qquad (3)$$

where H is the Heaviside unit step function, and the 'source function' G governs the profile of the incident wave. To model the instantaneous switching on of a time-harmonic plane wave of angular frequency $\omega > 0$ we take

$$G(t) = H(t) e^{-i\omega t}. \qquad (4)$$

A diagram showing the resulting wavefront configurations can be found in Fig. 1.

For large time we shall show that $\mathrm{Re}\,[\Phi]$ and $\mathrm{Im}\,[\Phi]$ are well approximated by the real and imaginary parts, respectively, of $\Phi_{\mathrm{freq}} = e^{-i\omega t}\phi$, where the 'limiting amplitude' ϕ is the solution of the corresponding frequency domain problem (here $k = \omega/c_0$)

$$\left(\nabla^2 + k^2\right) \phi = 0, \quad 0 < r < \infty, \quad 0 < \theta < 2\pi, \quad (5)$$

$$\frac{\partial \phi}{\partial \theta} = 0, \quad 0 < r < \infty, \quad \theta \in \{0, 2\pi\}, \quad (6)$$

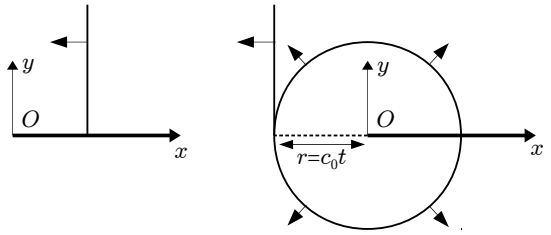

(a) $t < 0$ (b) $t > 0$

Figure 1: Wavefront configurations for the case $\theta_0 = 0^+$. The incident wavefront reaches the edge at $t = 0$, giving rise to a circular diffracted wavefront.

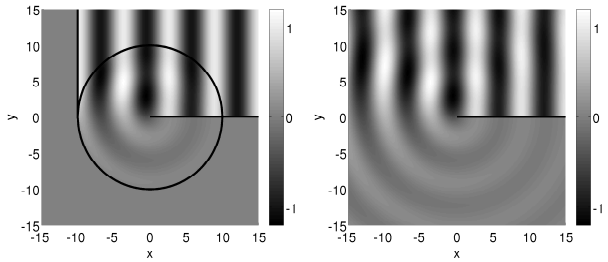

(a) $\mathrm{Re}[\Phi]$ (b) $\mathrm{Re}[\Phi_{\mathrm{freq}}]$

Figure 2: Field plots for the case $\theta_0 = 0^+$, with $\omega = 1$, $c_0 = 1$, $t = 10$.

along with the assumption that $\phi - H(\pi - \theta)e^{-ikx}$ should satisfy an outgoing radiation condition for $\theta \neq \pi$.

To be precise, defining $\delta\Phi := \Phi_{\mathrm{freq}} - \Phi$ and

$$\delta_{\mathrm{R}} := \frac{\mathrm{Re}[\delta\Phi]}{|\Phi_{\mathrm{freq}}|}, \qquad \delta_{\mathrm{I}} := \frac{\mathrm{Im}[\delta\Phi]}{|\Phi_{\mathrm{freq}}|},$$

we shall determine the conditions under which $\delta_{\mathrm{R}} \to 0$ and $\delta_{\mathrm{I}} \to 0$, as well as explicitly showing how the rate of convergence varies as a function of the observation point.

Analysis

The solution Φ of (1)-(3) is found by convolving the source function G with the solution Φ_δ of the 'impulse response problem', in which the source function is $\delta(t)$. Explicitly, with $\pm$ denoting $-\operatorname{sgn}(\pi - \theta)$, we have

$$\Phi_\delta = H(\pi - \theta)\delta\left(t + x/c_0\right) \pm \frac{H(t - r/c_0)}{2\pi} \frac{\sqrt{r(1+\cos\theta)}}{\sqrt{c_0 t - r}(t + \frac{r}{c_0}\cos\theta)}, \quad (7)$$

which can be obtained by differentiating with respect to t the response to an incident step discontinuity (source function $H(t)$), as derived in [7]. (Note that assigning $H(0) = 1/2$ ensures that (7) is analytic in $0 < r < c_0 t$, $\theta \neq 0, 2\pi$.) With G defined as in (4) we then have

$$\Phi = H(\pi - \theta)H(\xi^{\mathrm{inc}})e^{-i\xi^{\mathrm{inc}}} \pm \frac{H(\xi)\sqrt{\eta}}{2\pi} \int_0^\xi \frac{e^{i(s-\xi)}}{\sqrt{s}(s+\eta)}\, ds, \quad (8)$$

in terms of the nondimensional variables $\xi^{\mathrm{inc}} = \omega t + kx = \omega(t + x/c_0)$, $\xi = \omega t - kr = \omega(t - r/c_0)$ and $\eta = kr(1 + \cos\theta) = \omega r(1 + \cos\theta)/c_0$. The variables ξ^{inc} and ξ represent 2π times the number of periods of oscillation that have elapsed since the arrivals of the incident and diffracted wavefronts respectively. The variable η provides a measure of how close the observation point is to the shadow boundary $\theta = \pi$ of the frequency domain problem. Curves of constant η are parabolae with focus at the origin and axis along the shadow boundary (which corresponds to $\eta = 0$).

Behaviour close to the leading wavefront

In the illuminated region $\theta < \pi$ the leading wavefront is the incident wavefront $\xi^{\mathrm{inc}} = 0$, and, to leading order,

$$\left.\begin{aligned} \mathrm{Re}[\Phi] &\sim H(\xi^{\mathrm{inc}}), \\ \mathrm{Im}[\Phi] &\sim -H(\xi^{\mathrm{inc}})\,\xi^{\mathrm{inc}}, \end{aligned}\right\} \quad \xi^{\mathrm{inc}} \to 0, r > c_0 t.$$

Note that $\mathrm{Re}[\Phi]$ undergoes a jump discontinuity across $\xi^{\mathrm{inc}} = 0$, whereas $\mathrm{Im}[\Phi]$ is continuous, with $\frac{\partial \mathrm{Im}[\Phi]}{\partial \xi^{\mathrm{inc}}}$ undergoing a jump discontinuity.

In the shadow region $\theta > \pi$ the leading wavefront is the diffracted wavefront $\xi = 0$, and, to leading order,

$$\left.\begin{aligned} \mathrm{Re}[\Phi] &\sim \tfrac{H(\xi)}{\pi\sqrt{\eta}}\xi^{1/2}, \\ \mathrm{Im}[\Phi] &\sim -\tfrac{2H(\xi)}{3\pi\sqrt{\eta}}\xi^{3/2}, \end{aligned}\right\} \quad \xi \to 0,\ \xi \ll \eta. \quad (9)$$

In both $\mathrm{Re}[\Phi]$ and $\mathrm{Im}[\Phi]$ the strength of the singularity on the diffracted wavefront is weaker than that on the incident wavefront by half a power of ξ, which is a general principle of edge diffraction (see [8] for further discussion).

Convergence to the frequency domain solution

The solution of the frequency domain problem (5)-(6) is (see e.g. [9], p. 556)

$$\Phi_{\mathrm{freq}} = \frac{e^{-i(\omega t + kx + \pi/4)}}{\sqrt{\pi}} \int_{-\sqrt{2kr}\cos\frac{\theta}{2}}^{\infty} e^{is^2}\, ds. \quad (10)$$

For reference, example plots of $\mathrm{Re}\left[\Phi\right]$ and $\mathrm{Re}\left[\Phi_{\mathrm{freq}}\right]$ for fixed t can be found in Fig. 2. Plots of Φ, Φ_{freq} and the wavefront approximation (9) as functions of t, with the other parameters fixed, can be found in Fig. 3. Plots of $|\delta_{\mathrm{R}}|$ and $|\delta_{\mathrm{I}}|$ for fixed t can be found in Fig. 4.

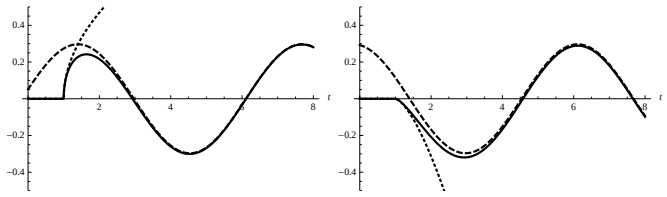

(a) real part (b) imaginary part

Figure 3: Comparison of Φ (solid), Φ_{freq} (dashed) and the wavefront approximation (9) (dotted) for the case $\theta_0 = 0^+$, with $\omega = 1$, $c_0 = 1$, $r = 1$, $\theta = \pi + 1$.

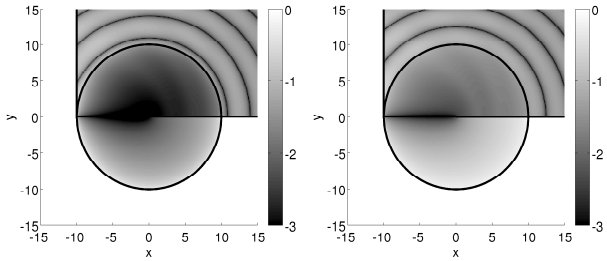

(a) $\log_{10}|\delta_{\text{R}}|$ (b) $\log_{10}|\delta_{\text{I}}|$

Figure 4: Logarithmic plots of $|\delta_{\text{R}}|$ and $|\delta_{\text{I}}|$ in the region behind the leading wavefront for the case $\theta_0 = 0^+$, with $\omega = 1$, $c_0 = 1$, $t = 10$.

To allow analytical progress in studying δ_{R} and δ_{I} we rewrite (10) in a form similar to (8). Using well-known properties of the Fresnel integral along with the identity

$$\int_{\sqrt{\eta}}^{\infty} e^{is^2}\,ds = \frac{\sqrt{\eta}e^{i(\eta+\pi/4)}}{2\sqrt{\pi}} \int_0^{\infty} \frac{e^{is}}{\sqrt{s}(s+\eta)}\,ds, \quad \eta > 0,$$

we obtain the representation

$$\Phi_{\text{freq}} = H(\pi-\theta)e^{-i\xi^{\text{inc}}} \pm \frac{\sqrt{\eta}}{2\pi} \int_0^{\infty} \frac{e^{i(s-\xi)}}{\sqrt{s}(s+\eta)}\,ds. \tag{11}$$

Comparing (8) and (11), we see that

$$\delta\Phi = \pm\frac{\sqrt{\eta}}{2\pi} \int_{\xi}^{\infty} \frac{e^{i(s-\xi)}}{\sqrt{s}(s+\eta)}\,ds, \qquad \xi > 0,$$

and repeated integration by parts gives

$$\left.\begin{aligned} \text{Re}[\delta\Phi] &\sim \pm\frac{\sqrt{\eta}(3\xi+\eta)}{4\pi\xi^{3/2}(\xi+\eta)^2}\left(1+O\left(\tfrac{1}{\xi^2}\right)\right), \\ \text{Im}[\delta\Phi] &\sim \pm\frac{\sqrt{\eta}}{2\pi\sqrt{\xi}(\xi+\eta)}\left(1+O\left(\tfrac{1}{\xi^2}\right)\right), \end{aligned}\right\} \quad \xi \to \infty,$$

uniformly for all $\eta > 0$.

This implies, for example, that for a fixed observation point (i.e. for kr and $\theta \neq \pi$ fixed, so that $\eta = O(1)$)

$$\delta_{\text{R}} = O\left(\frac{1}{\xi^{5/2}}\right), \quad \delta_{\text{I}} = O\left(\frac{1}{\xi^{3/2}}\right), \quad \xi \to \infty.$$

Analysis of the near-field ($\eta \ll 1$) and far-field ($\eta \gg 1$) regimes (see [5] for details) leads to the complete set of convergence results in Table 1. The key observations are:

1. The convergence of $\text{Re}[\Phi]$ is faster than that of $\text{Im}[\Phi]$ in the limit $\xi \to \infty$. This must be due to the stronger singularity on the incident wavefront.

2. The convergence is nonuniform in space, being fastest near the shadow boundary ($\eta \ll 1$). On the shadow boundary itself we have $\eta = 0$, so that $\delta\Phi = 0$, and the frequency domain solution is immediately attained once the leading wavefront has arrived, with

$$\Phi = \Phi_{\text{freq}} = \frac{1}{2}e^{-i\xi^{\text{inc}}}, \qquad \theta = \pi,\ t > r/c_0.$$

3. In the far-field ($\eta \gg 1$) the convergence is faster in the illuminated region than in the shadow region (cf. the asymmetry observed in Fig. 4).

The case $\theta_0 \neq 0$

We now consider the case of non-grazing incidence. For brevity we present only the case $0 < \theta_0 < \pi/2$, for which (3) must be replaced by

$$\Phi = \sum_{\pm} H(\pi - (\theta \pm \theta_0))G(t + (r/c_0)\cos(\theta \pm \theta_0)), \quad t < 0,$$

where $\sum_{\pm}$ represents the sum of the $+$ and $-$ terms.

The time-harmonic solution Φ_{freq} is now the sum of two terms, each associated with one of the two shadow boundaries $\theta = \pi \pm \theta_0$, each being of the form (11), but with θ replaced by $\theta \pm \theta_0$, and ξ^{inc}, η replaced by

Size of η	Size of ξ	Size of δ_{R}	Size of δ_{I}
$\eta \ll 1$	$\xi = O(\eta)$	No convergence	$O\left(\sqrt{\eta}\right)$
	$\eta \ll \xi = O(1)$	$O\left(\sqrt{\frac{\eta}{\xi}}\right)$	$O\left(\sqrt{\eta}\right)$
	$\xi \gg 1$	$O\left(\frac{\sqrt{\eta}}{\xi^{5/2}}\right)$	$O\left(\frac{\sqrt{\eta}}{\xi^{3/2}}\right)$
$\eta = O(1)$	$\xi \gg 1$	$O\left(\frac{1}{\xi^{5/2}}\right)$	$O\left(\frac{1}{\xi^{3/2}}\right)$
$\eta \gg 1$	$1 \ll \xi = O(\eta)$	$O\left(\frac{1}{\xi^{3/2}}\right)$	$O\left(\frac{1}{\sqrt{\xi}}\right)$
$\theta > \pi$	$\xi \gg \eta$	$O\left(\frac{\eta}{\xi^{5/2}}\right)$	$O\left(\frac{\eta}{\xi^{3/2}}\right)$
$\eta \gg 1$	$\xi = O(1)$	$O\left(\frac{1}{\sqrt{\eta}}\right)$	$O\left(\frac{1}{\sqrt{\eta}}\right)$
$\theta < \pi$	$1 \ll \xi = O(\eta)$	$O\left(\frac{1}{\sqrt{\eta}\xi^{3/2}}\right)$	$O\left(\frac{1}{\sqrt{\eta}\sqrt{\xi}}\right)$
	$\xi \gg \eta$	$O\left(\frac{\sqrt{\eta}}{\xi^{5/2}}\right)$	$O\left(\frac{\sqrt{\eta}}{\xi^{3/2}}\right)$

Table 1: Convergence results for the case $\theta_0 = 0^+$.

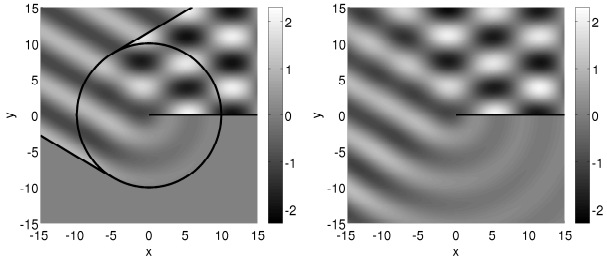

(a) Re[Φ] (b) Re[Φ_{freq}]

Figure 5: Field plots for the case $\theta_0 = \pi/3$, with $\omega = 1$, $c_0 = 1$, $t = 10$.

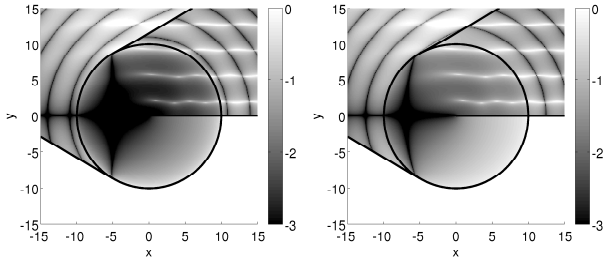

(a) $\log_{10}|\delta_{\text{R}}|$ (b) $\log_{10}|\delta_{\text{I}}|$

Figure 6: Logarithmic plots of $|\delta_{\text{R}}|$ and $|\delta_{\text{I}}|$ in the region behind the leading wavefront for the case $\theta_0 = \pi/3$, with $\omega = 1$, $c_0 = 1$, $t = 10$.

$\xi_\pm = \omega t + kr\cos(\theta \pm \theta_0)$, $\eta_\pm = kr(1 + \cos(\theta \pm \theta_0))$, respectively. Similarly, Φ is the sum of two terms of the form (8). Example plots of $\text{Re}\,[\Phi]$ and $\text{Re}\,[\Phi_{\text{freq}}]$ for the case $\theta_0 = \pi/3$ are presented in Fig. 5, and plots of δ_R and δ_I can be found in Fig. 6. The incident, reflected and diffracted wavefronts have been highlighted.

The convergence analysis of each of the two terms follows that of the case $\theta_0 = 0^+$, and we do not present the details here. There are, however, some important qualitative differences in the way that the time domain solution convergences to the frequency domain solution, as compared to the case $\theta_0 = 0$.

First, we note that the frequency domain solution is not instantaneously attained along either of the shadow boundaries $\theta = \pi \pm \theta_0$. This is because along either shadow boundary, one of the two terms making up Φ converges instantaneously, but the other does not. However, the convergence is immediate along the line $\theta = \pi$ (the continuation of the half-line into $x < 0$). Indeed, once the incident wavefront has arrived we have

$$\Phi = \Phi_{\text{freq}} = e^{-i\omega(t-(r/c_0)\cos\theta_0)}, \quad \theta = \pi,\ t > \frac{r\cos\theta_0}{c_0}.$$

Second, we remark on the 'tongue-like' features observed in the reflected region $0 < \theta < |\pi - \theta_0|$ in the relative error plots in Fig. 6. These are due to the effect of interference between the incident and reflected components of Φ_{freq}. Along the lines $y = (n+1/2)\pi/(k\sin\theta_0)$, $n = 0, 1, 2, \ldots$, the incident and reflected components of Φ_{freq} cancel exactly, so that Φ_{freq} comprises a (small) diffracted component in the far field. Close to these lines, δ_R and δ_I are similar in magnitude to what they are in the corresponding part of the shadow region (i.e. at angle $2\pi - \theta$). Away from these lines, as was found to be the case for $\theta_0 = 0^+$, δ_R and δ_I are smaller in the illuminated region than in the corresponding part of the shadow region.

Acknowledgements

D. P. Hewett acknowledges the support of the EPSRC and Dstl (MOD research contract RD023-2985).

References

[1] R. N. Buchal, "The approach to steady state of solutions of exterior boundary value problems for the wave equation", J. Math. Mech. 12 (2), pp. 225-234, 1963.

[2] C. S. Morawetz, "The limiting amplitude principle", Comm. Pure and App. Math. 15 (3), pp. 349-361, 1962.

[3] C. S. Morawetz, "The limiting amplitude principle for arbitrary finite bodies", Comm. Pure and App. Math. 18 (1-2), pp. 183-189, 1965.

[4] A. I. Komech and A. E. Merzon, "Limiting amplitude principle in the scattering by wedges", Math. Meth. Appl. Sci. 29, pp. 1147-1185, 2006.

[5] D. P. Hewett and J. R. Ockendon and D. J. Allwright, "Switching on a two-dimensional time-harmonic scalar wave in the presence of a diffracting edge", Wave Motion 48 (3), pp. 197-213, 2011.

[6] M. Abramowitz and I. A. Stegun, Handbook of Mathematical Functions, United States Department of Commerce, 1964.

[7] J. B. Keller and A. Blank, "Diffraction and reflection of pulses by wedges and corners", Comm. Pure and App. Math. 4 (1), pp. 75–94, 1951.

[8] D. P. Hewett, Sound propagation in an urban environment, DPhil thesis, University of Oxford, 2010.

[9] D. S. Jones, Acoustic and Electromagnetic Waves, Oxford University Press, USA, 1989.